Analysis of Cell Movement by Simultaneous Quantification of Local Membrane Displacement and Fluorescent Intensities Using Quimp2

Bosgraaf, Leonard; van Haastert, Peter J. M.; Bretschneider, Till

Published in:
Cell Motility and the Cytoskeleton

DOI:
10.1002/cm.20338

Publication date:
2009

Cell Motility and the Cytoskeleton 66: 156–165 (2009)

Analysis of Cell Movement by Simultaneous Quantification of Local Membrane Displacement and Fluorescent Intensities Using Quimp2

Leonard Bosgraaf,[1] Peter J.M. van Haastert,[1]* and Till Bretschneider[2]

[1]*University of Groningen, Cell Biochemistry Department, Haren, The Netherlands*

[2]*University of Warwick, Warwick Systems Biology Centre, Coventry, United Kingdom*

The use of fluorescent markers in living cells has increased dramatically in the recent years. The quantitative analysis of the images requires specific analysis software. Previously, the program Quimp was launched for quantitating fluorescent intensities at the membrane or the cortex of the cell. However, Quimp is not well suited to quantitate local membrane displacement. Here we present Quimp2 that is capable of tracking membrane subregions in time, which enables the simultaneous quantification of fluorescent intensities and membrane movement. Quimp2 has two new tools, (i) conversion filters to analyze movies obtained with fluorescent, DIC and phase contrast different microscopes, and (ii) a macro that calculates the local membrane displacement and provides various options to display the results. Quimp2 is used here to investigate the molecular mechanism of cell movement by correlating the dynamics of local membrane movement with the local concentration of myosin and F-actin. Cell Motil. Cytoskeleton 66: 156–165, 2009.

Key words: actin; myosin GFP; software; analysis; movement

INTRODUCTION

Cellular processes are mostly dynamic in nature. It is therefore not surprising that the use of fluorescent markers such as green fluorescent protein (GFP) has increased dramatically in the recent years. However, the development of software capable of quantitating fluorescent images or movies has been scarcely reported. One program that was developed for such purposes is Quimp (Quantitative Imaging of Membrane Proteins), which is suitable for proteins that reside in the membrane or cortex [Dormann et al., 2002]. This program uses an active contour method [Kass et al., 1987] to automatically recognize the outlines of a cell. For this, a manual chain selection encompassing the cell is required for the first frame. The program creates a number of interconnected nodes on this chain, based on a user-defined distance between nodes. Subsequently, this chain of nodes is shrunk towards the cell; if the distance between two nodes becomes closer than a user-defined distance, one of them is deleted. The nodes are fixed in space when a user-defined steepness in fluorescent signal (the cell boundary) is reached. The cell boundary is thus described by the position of the nodes. For subsequent movie frames, the chain of nodes of the preceding frame

Additional Supporting Information may be found in the online version of this article.

*Correspondence to: P. J. M. van Haastert, Department of Molecular Cell Biology, University of Groningen, Kerklaan 30, 9751NN Haren, The Netherlands. E-mail: P.J.M.van.Haastert@rug.nl

Received 30 September 2008; Accepted 8 December 2008

Published online 4 February 2009 in Wiley InterScience (www.interscience.wiley.com).
DOI: 10.1002/cm.20338

is enlarged, and new nodes are inserted between the old ones followed by a new round of chain shrinkage and cell boundary detection. After the cell has thus been tracked for the full movie, the membrane- or cortex fluorescent intensity is sampled for each node. This is accomplished by scanning a line segment pointing from the node towards the cell body for the maximum fluorescent value.

Although Quimp is well capable of quantitating the local fluorescent intensities, it is not well suited to determine the local movement of the membrane. For example, it is not possible to determine the speed of the nodes, since the nodes of two subsequent frames do not have a positional relationship. Here a new Quimp version is introduced, Quimp2, which assigns a tracking number to each node. Using these tracking numbers, the nodes can be followed in time, which enables the quantification of local membrane movement. Our approach to tracking cell boundaries is similar to the one based on a mechanical model of cell contours developed by [Machacek and Danuser, 2006]. The advantage of QuimP2 however is that cell edge detection and boundary tracking are performed in one step which makes the procedure very fast (about 1 s per frame) and that crossing-overs of adjacent nodes as seen in [Machacek and Danuser, 2006], are excluded. The currently probably most advanced software for cell motility and shape analysis is DIAS (Soll Technologies) and has been used widely for morphometric analysis of moving cells. Although QuimP is not yet advanced as DIAS in terms of user-friendliness our software is freely available as a set of plugins and macros for the popular ImageJ software toolkit and highly flexible. The unique feature of QuimP is that movement of the cell boundary can be correlated with local membrane fluorescent intensities, which is useful in studying the function of specific proteins for cell movement. We also present a newly developed macro, which performs a number of calculations for each node and supplies various ways to quantify and present the results. The new Quimp2 package can be a valuable set of tools to quantify and automate the analysis of localized protein behavior.

METHODS

Quimp2 is available as a plugin for the open source program ImageJ (http://rsb.info.nih.gov/ij/). A detailed description of the previously reported Quimp version can be found on this site: http://go.warwick.ac.uk/bretschneider/quimp and in the article describing the earlier Quimp version [Dormann et al., 2002]. The Quimp BOA plugin (for cell tracking) was modified such that each node was assigned a unique number (tracking number). For the first frame of the movie, node numbers are assigned after the first outline has been completed to ensure that the analysis starts with a well-defined sequence of node numbers. The positions of the nodes at frame t are used to determine the positions at frame t+1 in the following way: The chain is enlarged between successive frames to account for cell motion. This requires new nodes to be inserted as its length increases. Newly inserted nodes are assigned higher tracking numbers. The subsequent shrinking process to identify the cell boundary at frame t + 1 is performed iteratively by integrating a simple force balance equation [Dormann et al., 2002]. During this process nodes with higher tracking numbers are lost first when nodes come too close. Most of these nodes therefore can be considered as ''virtual nodes'' that do not actually appear in the final contour of the subsequent frame. They are inserted during blow-up of the chain between subsequent frames and deleted during shrinkage of the chain in the cell outline detection procedure. By applying this scheme we are able to connect most of the nodes at frame t with their corresponding nodes having the same tracking number at frame t + 1. The number of nodes that will be kept between frames depends on the extent of cell deformation. In retracting regions more nodes will be lost permanently in order to keep the node density roughly constant while in extending regions nodes will be added that are maintained until that region retracts. The chain is processed alternating clockwise and anti-clockwise to rules out a bias in the selection process of nodes to be inserted or deleted. The plugin was renamed BOA_TN and creates a data file containing the tracking number data. The Quimp ANA plugin (for intensity sampling) was modified accordingly, and the novel ANA_TN plugin writes the tracking number of each node to a data file, as well as all the other required parameters (x- and y-coordinates, fluorescence intensities, etc.; see Table I of Supp. Info.). In the standard setting the average distance between nodes is 0.45 μm; with a cell perimeter of 75 μm this yields about 170 nodes.

Retraction and Extension Areas of the Cell

In order to extract more information from the raw data, a novel macro was developed. Although macros run somewhat slower than plugins in ImageJ, the macro language is quite simple, which simplifies modification by other users. The tracking number analysis macro calculates a number of parameters for each node. The displacement of the nodes is always calculated from their positions in the previous frame to their positions in the next frame. One important parameter that is calculated is whether the node is in an extending or in a retracting area. In Fig. 1 a schematic drawing of a moving cell is shown. The nodes are represented as black dots. The movement of two nodes is highlighted by displaying their positions in the previous and next frames. Clearly, the position of the retracting node in the next frame is

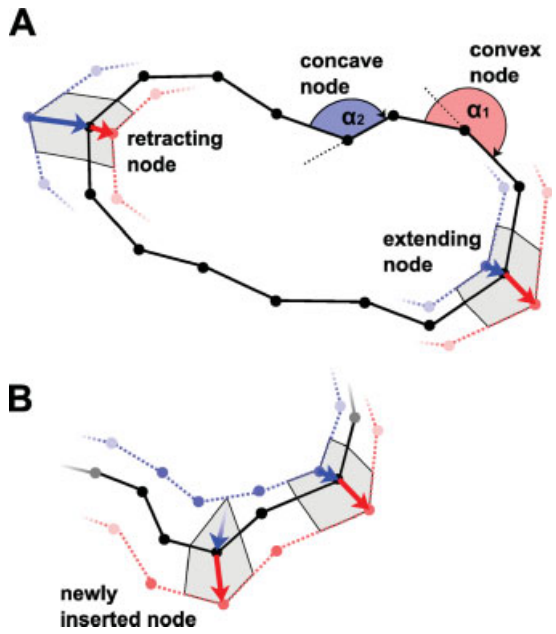

Fig. 1. Schematic drawing of a cell traced by Quimp. The figure displays the chain of interconnected nodes for a single frame in black and some nodes of the previous frame in blue. Note that the amount of nodes is much higher in praxis (typically 130–180 per frame). Panel **B** shows part of a chain with an inserted node. The ''extending node'' at the right side of the image depicts a node that is in an extending area. The movement of the node from the previous frame (blue line) to the current frame is indicated with a blue arrow, whereas the red arrow indicates the displacement of the node from the current frame to the next frame (red line). The position of the node in the next frame is outside the chain of the previous frame. This property is used as the criterion to define it as an extending node. Similarly, the position of the ''retracting node'' in the next frame is enclosed in the chain of the previous frame. The area surrounding the node is drawn in gray for two nodes. It is defined by the points that lie halfway the node of interest and its neighbors, for the previous, current and next frame. This area is used to express the movement of the area represented by the node as ''area change,'' which is the gained or lost area in μm^2 per second. The local curvature of the cell boundary is determined for each node. In this figure, a concave and a convex node are highlighted. For the concave node, the outer angle α of the line segments connecting the node with its neighboring nodes is smaller than 180°; for the convex node, this angle α is larger than 180°. Note that the chain of nodes forms a closed polygon. Therefore, in a perfectly round cell all the nodes would be assigned convex. To correct for this, the value ''360/number of nodes'' is subtracted from the calculated angles.

inside the cell boundary of the previous frame (i.e., the red dot of the retracting node is inside the blue line). As opposed to this, the position of the extending node is outside the outline of the cell in the previous frame (i.e., the red dot of the extending node is outside the blue line). The magnitude of the retracting/extension can be expressed as speed of the node, by dividing the displacement of the node by the amount of seconds per frame. However, if the movement of a node is primarily parallel to the membrane, this can give erroneous results, because the speed is high while there is minimal retraction or extension. This problem is circumvented by using the area represented by the node (gray area in Fig. 1) in stead of the displacement of the node. In case the node is moving parallel to the membrane, this area change is very small. The area change was calculated as follows (see Fig. 1): for a specific node the points halfway the two adjacent nodes was determined for the present, previous and next frame. The area change of the node in the present frame is half the surface area covered by these points. The extension/retraction parameter is used as a sign (minus for retraction, plus for extension) in front of the area change of the node. Thus, a highly negative area change indicates a strongly retracting node, whereas a highly positive area change represents a strongly extending node.

A special area of retraction is the uropod in the rear of the cell, which can be detected in two ways. After the movie is loaded, the user is asked to identify approximately where the uropod is at the beginning of the movie with a mouse click. The central uropod node of subsequent frames is identified by the node with maximal retraction in the area of the previous uropod. This method works very well if the uropod remains in the ''back'' half of the cell. In case the cell does make head to tail conversions (which does happen in shortly starved cells) the user can choose an alternative, fully automatic and dynamic method of uropod tracking that works well in most cases: The macro gives the option to mark the central node of the uropod throughout the entire movie. The uropod is used to define the polarity axis of the cell. The central uropod node is the ''rear'' of the cell, while the node furthest apart from this central uropod node (as measured along the perimeter) is defined as the ''front''.

Concave and Convex Areas of the Cell

The local curvature of the cell outline was used to further define specific regions of the cell. The angle α of the line segments pointing from a given node to its two neighbors was used for this purpose. If the angle is larger than 180°, the node is assigned ''convex'', if it is smaller than 180° it is a ''concave'' node (see Fig. 1). The angle is corrected by subtracting $360/n$ for the fact that the chain of n nodes forms a closed polygon. Thus, the curvature c is given by $c = \alpha - 180 - 360/n$. Positive and negative values of c imply convex and concave nodes, respectively.

Recording of Movies

The movie for the analysis of myosin and actin in cell protrusions (Figs. 3–7) was made as follows. Wild type *Dictyostelium discoideum* AX3 amoeba carrying the LB15B plasmid were grown on a coated Petri dish (Nunc) with 10 ml HG5 medium supplemented with

10 μg/mL hygromycin. The LB15B plasmid carries the full myosin II heavy chain open reading frame fused at the N-terminus with the gene encoding mRFP-mars [Fischer et al., 2004]. Furthermore, it also contains the F-actin binding domain (amino acid 1-145) of LimE [Prassler et al., 1998], which is C-terminally fused to the GFP-S65T gene. The cells were starved in 10 mM phosphate buffer (pH 6.5) until the onset of aggregation (about 5 h) and placed in an Ibidi perfusion chamber. At the indicated time point, 200 μL of a 10^{-6} M cAMP solution was added to the cells. Fluorescent images for red and green fluorescence were simultaneously recorded at 4 s time intervals using a Zeiss 510 inverted confocal laser scanning microscope.

RESULTS AND DISCUSSION

Quimp2

The previously described Quimp program consists of a set ImageJ plugins that was developed to quantitate fluorescence intensities at the membrane or cortex [Dormann et al., 2002]. The program defines the outline of the cell by a chain of interconnected nodes. In the standard setting we use an average distance between nodes of 0.45 μm; with a cell perimeter of 75 μm this yields about 170 nodes. To each node, the position and local fluorescence intensity values are assigned. We extended the programs capabilities by assigning a unique tracking number to each node. By analyzing the position of the nodes in time, the movement of the nodes can then be quantified.

The macros and plugins of the new Quimp package can be launched by an action bar, that include the BOA_TN plugin to track the cell boundary and the ANA_TN plugin to sample the fluorescent intensities (Fig. 2). The three most important parameters that are determined for each node are: the direction of movement (retracting or extending), the area change (the area that is lost or gained per second at the membrane segment that is represented by the node) and the convexity/concavity of the outline (see methods section for details). The area change can be thought of as the speed of the node in two dimensions (its unit is $\mu m^2/s$).

Fig. 2. The Quimp2 action bar. Screenshot of the action bar of the Quimp2 package. The action bar was created with Jerome Mutterer's ImageJ plugin. The buttons activate the following components (from left to right): 1. The BOA_TN plugin to track the cell boundary; 2. The ANA_TN plugin to sample the fluorescent intensities; 3. The tracking number analysis macro to perform additional calculations; 4. Macro to apply the custom blue-red hot LUT for re-opened 32-bit images; 5. Macro which runs a number of filters to convert DIC movies to black and white; 6. Macro which runs a number of filters to convert phase contrast movies to black and white; 7. Macro to convert fluorescent movies to black and white (may be useful in case of problematic tracking); 8. The manual is displayed. [Color figure can be viewed in the online issue which is available at www.interscience.wiley.com]

F-actin and Myosin in Regions of Extension and Retraction

To demonstrate the power of the program and to analyze the role of myosin and actin in cell movement, *Dictyostelium discoideum* amoebae were used that express two fluorescent cytoskeleton markers. These are the conventional myosin II heavy chain fused to the monomeric red fluorescent protein mars [Fischer et al., 2004] and the filamentous actin-binding domain of LimE fused to GFP [Prassler et al., 1998]. After starvation, *Dictyostelium* cells become sensitive to cAMP, which serves as a chemoattractant. Starved cells were allowed to move in buffer and then subjected to a sudden global increase of cAMP, which leads to translocation of the cytoskeleton markers to the cortex. A confocal laser scanning microscope was used to capture images at 4 s interval. The movie was subsequently analyzed with the plugins of the Quimp package. In Fig. 3, eight stills of the movie are shown, whereas the full movie is available as supplemental data (movie S1). The left and middle panels present F-actin and myosin, respectively, while the local area change of the membrane is presented in the panels at the right. The stills of F-actin and myosin show that just before stimulation (time point −8 s), F-actin is found primarily in extending pseudopodia, whereas myosin II is often enriched in retracting pseudopodia and the uropod. Upon cAMP addition, the cell freezes for about 40 s (compare the cell shape of time points 0–28 in Fig. 3). Furthermore, a strong global increase of F-actin at the cortex follows at 4–12 s after stimulation (see 8 s time point in Fig. 3). A less profound translocation of myosin to the cortex occurs at 24–32 s after stimulation. A second F-actin boost starts after 52 s and is accompanied by the formation of two new pseudopodia (yellow arrows in 60 s time point). One of the pseudopodia is retracted around 96 s and the typical F-actin- and myosin distribution is resumed from there on.

One of the output files of the macro is an ''outline movie''. This type of movie is created by interconnecting the nodes with line segments for each frame. The color of the line segments corresponds to a user-specified feature. In Fig. 3 (right columns), the area change was chosen for this purpose. Blue areas denote regions of retracting membrane, whereas red areas are extending. The lightness of the color indicates the speed of area change. At time point −8 s, for example, the yellow-orange region at the bottom of the cell is strongly extend-

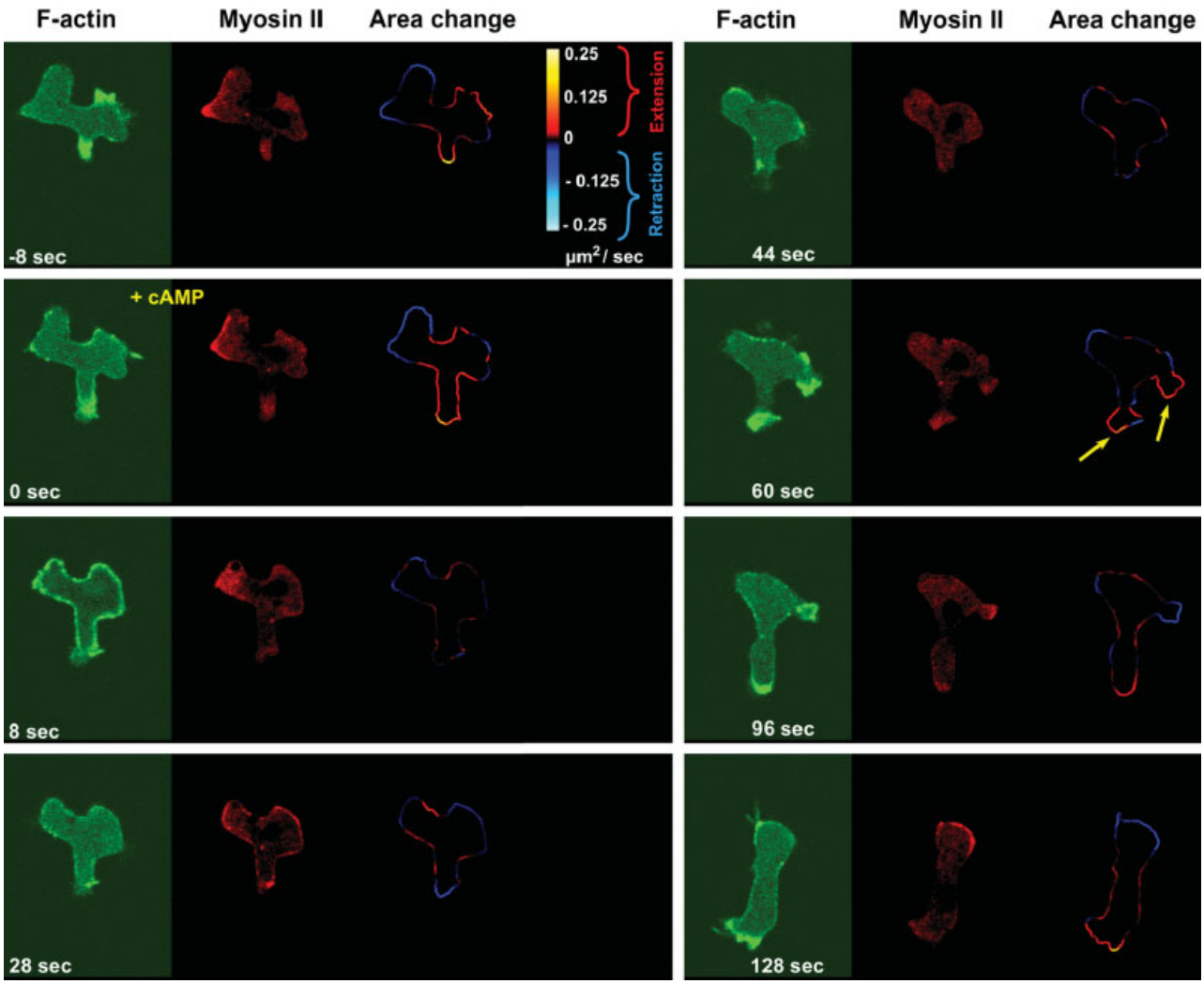

Fig. 3. Chemoattractant-induced myosin- and actin responses and local membrane movement. Starved wild type *Dictyostelium* cells expressing red fluorescent myosin II and a green fluorescent F-actin label (the actin binding domain of LimE) were subjected to a global cAMP stimulation at time point 0. The images are stills taken from the original fluorescent movies (columns labeled with F-actin and Myosin II) and from an outline movie that was created with the tracking number analysis macro (column labeled Area change). The full movie is available as supplementary data (Supp. Info. Movie S1). Shortly after the cAMP stimulation, a strong increase in cortical actin filaments is observed (8 s). A second F-actin boost is visible at 60 s, which is accompanied by the formation of two new pseudopodia (yellow arrows). Subsequently, the normal localization of F-actin and myosin is restored. The less pronounced myosin II translocation occurs between the two actin boosts (28 s). The area change pictures visualize the local displacement of the cell boundary; the calibration bar indicates the meaning of the colors. Note the abundance of F-actin in extending regions and the enrichment of myosin II in retracting regions before stimulation (−8 s), and the dramatic drop of the extension- and retraction activities after cAMP stimulation (8–44 s).

ing, whereas the blue areas are retracting. Note that these regions are enriched in F-actin and myosin, respectively. At 8 s after stimulation, the inactive state of the cell is clearly visible by the dark colors of the outline, which indicate slow node movement.

The tracking number analysis macro also creates a cell track, which consists of the outlines of the cell stacked on top of each other. In Fig. 4A, the cell track is created with time driven coloring, which gives a global idea of the cells' movement during the course of the movie. Figures 4B–4D are three examples of 2D plots that can also be created by the macro. In this type of plot, each row represents one frame and each pixel represents the data of one node. It can be depicted as the cell perimeter that is cut open and straightened for each consecutive frame, going further in time from top to bottom. The value of the pixel is determined by a certain feature, which can be chosen by the user.

In Fig. 4B, the area change is displayed, whereas Figs. 4C and 4D show the intensities of the F-actin stain and myosin II, respectively. In Fig. 4B, the freezing of the cell just after cAMP stimulation is clearly visible by

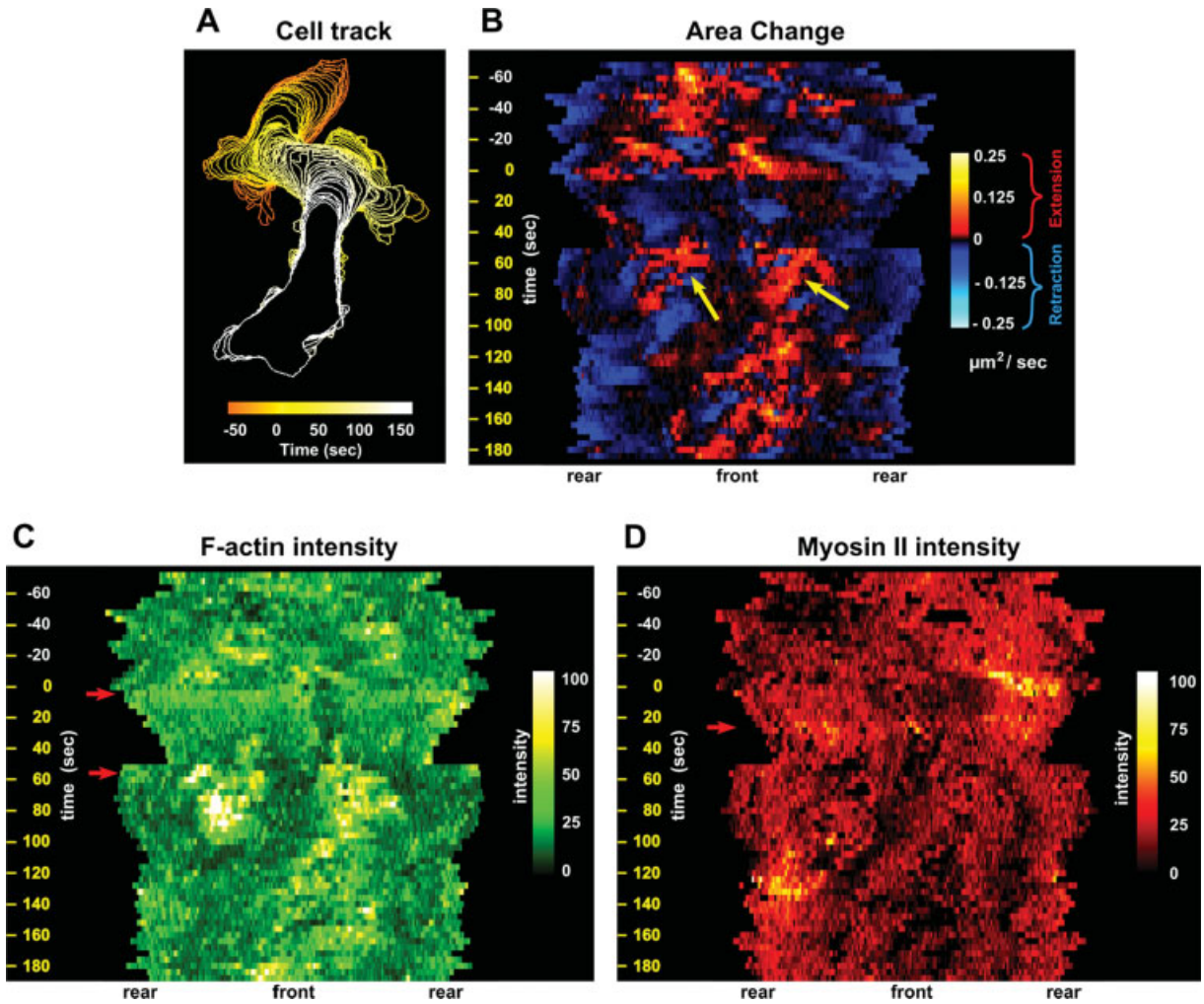

Fig. 4. Cell track and 2D plots created by Quimp2. The movie introduced in figure 3 was analyzed with the Quimp2 package. The resulting cell track is shown in panel **A**. The cell track is composed of the stacked outlines of the cell, starting at the first frame. The individual outlines are created by connecting the positions of the nodes. In this example, the coloration is time-driven. Three 2D plots are presented as panels **B–D**. 2D plots can be depicted as the linearized perimeter of the cell that is plotted for each frame, starting at the top. Each pixel represents one node, thus the width is proportional to the perimeter of the cell (the upper line in panels C and D, representing the first frame, has 136 nodes and a perimeter of 60 µm). The color of the pixels depends on a user defined property, such as node displacement (panel B) or fluoresencent intensity (F-actin in panel C and myosin in panel D). Note the absence of extending areas shortly after cAMP-stimulation and the formation of two novel pseudopodia (yellow arrows) at around 50 s after cAMP stimulation in panel B. In panel C, the first actin boost (upper arrow) is much more homogeneous than the second (lower arrow). The myosin translocation is less pronounced, but is still clearly visible in panel D at the position of the arrow. The much stronger myosin enrichments at −5 s and 130 s coincide with strongly retracting areas.

the darker coloration of the plot from time point 4 to 40 s. During this time period, the cell displays very little extension. In contrast, contraction does continue, albeit at lower rates. This can be readily seen by the steady decrease in the cell's perimeter and in the number of nodes, which causes the 2D plots to narrow. At around 50 s, the two newly created pseudopodia (yellow arrows) can be observed as two orange areas on the 2D plot. One of these is retracted (which is visible by the blue area below the left orange area), whereas the other continues to grow. In Fig. 4C the first global F-actin boost is clearly visible as a quite homogeneous green band (upper arrow). The second boost (lower arrow) only occurs in two regions that coincide with the position of the pseudopodia. The cAMP-induced myosin II translocation can be observed in Fig. 4D (red arrow). The translocation is more heterogeneous than the first F-actin boost, and is also less clear. Interestingly, the typical cringe of the cell is already halfway before the myosin translocation occurs. Moreover, the translocation of myosin does not seem to increase the speed of retraction much (see below). These observations suggest that the

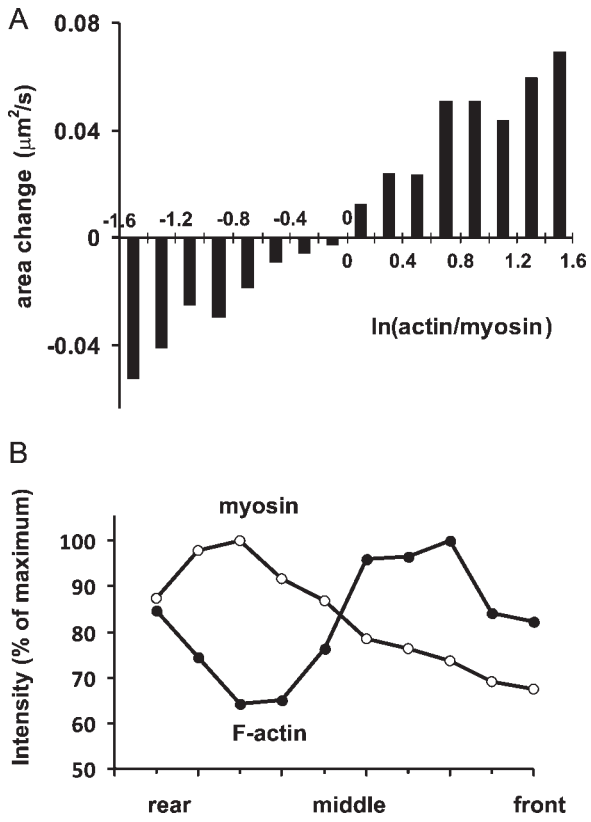

Fig. 5. Global analysis of movement and cortex intensities. **A:** correlation between F-actin/myosin and extension/retraction. The actin and myosin values are fluorescence intensities of LimE-GFP (actin) and myosin-RFP, respectively, and were normalized to the average of all nodes of all frames. The extension speed of all 10,532 nodes is plotted against the ratio of F-actin/myosin; the logarithm of this ratio is plotted to obtain an equal value for $\ln(x)$ and $-\ln(1/x)$. The results show that extending nodes are enriched in F-actin, while retracting nodes have more myosin. **B**: Averaged cortex intensities from rear to front. The location of myosin and F-actin was visualized by plotting the averaged data of the data file, which was created by Quimp2. In this data file, the nodes are separated in 10 groups by means of their distance to the rear of the cell. The average fluorescence intensity of each group is calculated for each frame. The data points of this graph were obtained by averaging the values per group over the entire movie. The enrichment of myosin in the rear of the cell and the higher concentration of actin filaments in the front is readily visible. F-actin is also enriched in the rear of the cell, which is caused by the bright non-protruding actin spots that are often observed in the back of the cell.

cringe of the cell may not be caused by the translocation of myosin II to the cortex.

One important practical feature of the 2D plots is that they are created as 32-bit files, which, in contrast to 8-bit files, allows for negative values. In addition, pixels that do not represent a node have the value NaN (not a number), and are not considered in ImageJ measurements. Moreover, the pixel values are exactly equal to the calculated values, making the 2D plots suitable for further analysis. For example, an extending area may be chosen as region of interest from Fig. 4B, and the corresponding F-actin intensity can be easily determined by measuring the mean intensity of that same region in Fig. 4C.

Quantitative Analysis of Cell Movement and Fluorescence Intensities of F-actin and Myosin II

Apart from the outline movie and the 2D plots, the tracking number analysis macro also exports a number of text files. These files can be used for further analysis, for example by importing them in a spreadsheet program. We have used these data files for global analysis and correlation of cell movement with fluorescent intensities, and subsequently to inspect movement and intensities of specific nodes or frames of the movie. One of the text files (dat5) contains the primary data on x,y-positions and fluorescence intensities for all nodes of all frames, as well as the deduced data on extension, retraction, speed, and convexity of the nodes. Figure 5A presents the correlation between extension/retraction and F-actin/myosin for all 10,532 nodes of the movie, clearly demonstrating that extending areas of the cell are enriched in F-actin, while retracting areas contain more myosin II.

The localization of proteins within a moving cell can also be quantitated relative to the polarity axis of the cell. The uropod of the cell is tracked by the macro during the entire movie. The rear of the cell is defined as the central uropod node. The ''front'' is defined as the node furthest apart from this central uropod node. A separate text file (dat7) is made in which the nodes are grouped according to their distance from the rear along the cell perimeter, providing a front-rear polarity axis of the cell. Figure 5B contains the intensity data of myosin and F-actin for the grouped nodes, averaged for the entire movie. This graph clearly shows the enrichment of myosin in the rear of the cell and the preferential formation of actin filaments in the front of the cell. Furthermore, the F-actin label is also enriched in the rear of the cell, comprising acto-myosin, which was observed before [Yumura et al., 1984; Yumura, 1994].

Another text file (dat6) contains for each frame the values of many properties, averaged over all the nodes in that frame; these properties include cell surface area, cell perimeter, gained area, lost area, net area change, speed and fluorescence intensities of the cortex, but also correlation coefficients between area change and cortical intensities. This file is very convenient to analyze temporal responses. Figure 6A shows the averaged fluorescence intensities of myosin II and the filamentous-actin label. The spread (standard deviation) is visualized by a lighter area underneath the data line. The two actin boosts and the myosin translocation are clearly visible and exhibit similar kinetics as shown before [McRobbie

and Newell, 1983, 1984; Berlot et al., 1987; Hall et al., 1988; Yumura, 1994; Chen et al., 2003; Etzrodt et al., 2006]. Furthermore, the spread of the intensity is much smaller for the first actin boost compared to the second. The area changes of extending and retracting nodes are summed separately in the text files. This can be very useful to quantify the amount of extension and retraction of the cell at different time points (Fig. 6B). Before cAMP addition, the extension and retraction activity of the cell vary in time, but averaged over a longer time interval extension and retraction are approximately equal (~ 2 $\mu m^2/s$). Immediately after addition of cAMP, the extension and retraction activity of the cell collapses. However, the extension drops to 0.54 $\mu m^2/s$, whereas the retraction rate is still -1.3 $\mu m^2/s$ on average. Since this period lasts about 40 s, this means that the cell should lose an area of about 30 μm^2. Indeed, the area of the cell goes from 170 μm^2 to 140 μm^2 in this time period. Note that the extension and retraction rates are quite constant during this period.

In Fig. 6C, the correlation coefficients between the area change and the fluorescent intensities are plotted. The correlation coefficient can be used as a measure for the strength and direction of a relationship between two data sets and ranges from -1 to 1. We first describe the correlations before and long (>40 s) after cAMP stimulation. Clearly, the myosin II intensity has a negative correlation with the area change, meaning that it is enriched in retracting areas. The F-actin label intensity displays a positive correlation with the area change, though it is less profound. This could be due to the F-actin spots that can be regularly observed in the rear and lateral cortex of the cell (see for example the 128 s time point of Fig. 3). In contrast, between 4 and 40 s after cAMP stimulation the correlation coefficient between area change and F-actin drops to zero, which confirms that the formation of actin filaments is not coupled to membrane movement during the first F-actin response. During this period, myosin translocates to the cortex, and the maximum of myosin translocation at 28 s correlates with enhanced retraction. In contrast to the first

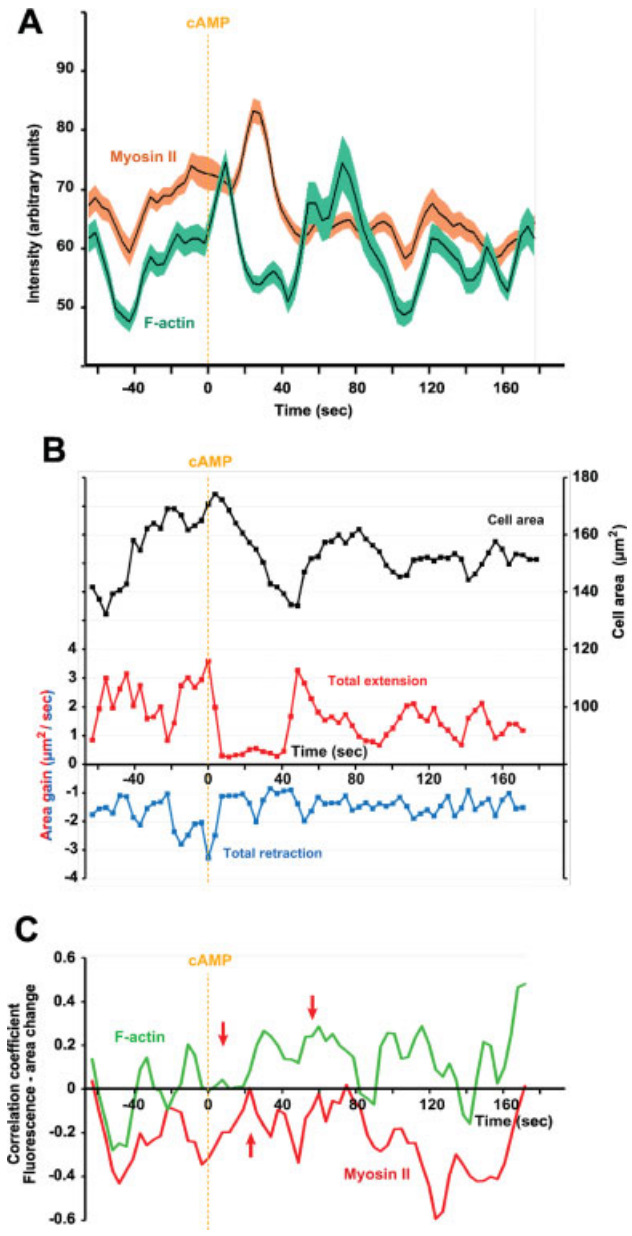

Fig. 6. The progression of the mean fluorescent intensities and the movement of the cell perimeter. Quimp2 exports a data file with the means and standard deviation of various properties per frame. The figure presents fluorescent intensities and area changes. In panel **A**, the average cortex intensities of myosin II and the F-actin are plotted (solid lines). The lighter colored area surrounding the lines is the standard error of the mean. Note that during the first F-actin boost (5 s), the standard error is much smaller (i.e., a more uniform distribution of F-actin at the membrane) than during the second boost (i.e., F-actin in pseudopod patches at 50 s). The myosin translocation occurs at around 30 s. In panel **B**, the total gained area and the total lost area are plotted on the left axis, whereas the area of the cell is plotted on the right axis. Note that immediately upon cAMP addition, both the retraction and extension rates drop. The observed decrease of the cell area apparently does not result from a sudden strong retraction, but rather from a 40 s period of very little extension and moderate retraction. Furthermore, the retraction is only mildly effected by the myosin II translocation. In panel **C**, the relationship between local intensities and movement is visualized by plotting the Pearson product-moment correlation coefficient. The values are averaged over three frames to reduce noise. A positive correlation coefficient means the intensity is significantly higher in extending areas. As expected, the F-actin label intensity displays a positive correlation with the area change, whereas myosin is negatively correlated with the area change. The two F-actin boosts and the myosin translocation are indicated by arrows. Note that the correlation coefficient of F-actin drops to zero during the first boost, which implies that the formation of actin filaments is not coupled to membrane displacement at this point. [Color figure can be viewed in the online issue which is available at www.interscience.wiley.com].

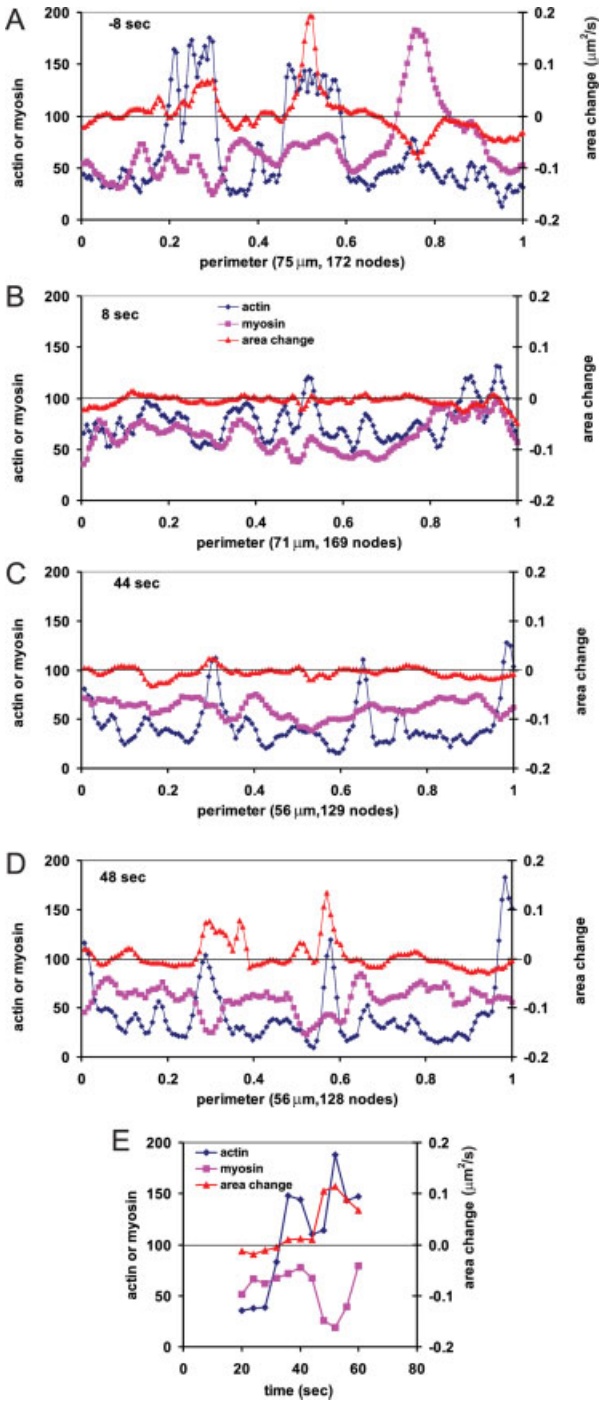

Fig. 7. Movement and cortex intensities of the nodes in specific frames of the movie. The fluorescence intensities of the cortex for F-actin and myosin II, and the area change are presented for all nodes of the frames indicated. The perimeter of the cell is scaled to 1 in all frames; the perimeter in μm and the number of nodes is indicated in the figure. Panel **E** presents the cortical intensities and area change of the nodes that comprise the pseudopodia that emerge at 52 s as function of the time after cAMP stimulation. The figure reveals that F-actin accumulates long before the pseudopod is extended, and that the extensions at 48 s coincide with the local depletion of myosin from the cortex. [Color figure can be viewed in the online issue which is available at www.interscience.wiley.com].

actin boost, the second F-actin boost around 60 s displays a clear positive correlation between area change and F-actin, which is obviously the result of the extension of the heavily F-actin filled pseudopodia.

The detailed dat5 file that contains all information was used to inspect in detail the potential temporal-spatial connection between local F-actin/myosin intensities and extension/retraction area. In Fig. 7 we present the area change, and fluorescence intensities of F-actin and myosin II for the nodes of the frames presented above in Fig. 3. Before cAMP stimulation (−8 s, Fig. 7A) two regions of extension are present, which are both associated with elevated levels of F-actin. One region of the cell that is retracted exhibits strongly increased levels of myosin II; interestingly, this region shows also elevated F-actin levels, confirming that retraction is mediated by acto-myosin [Yumura et al., 1984; Yumura, 1994]. The average level of F-actin in regions of the cells that are not extended or retracted is about 35 (in arbitrary units). The cell image taken at 8 s after cAMP stimulation (Fig. 3) revealed strong translocation of LimE-GFP to the entire cortex. The quantitative data (Fig. 7B) reveal that the arbitrary F-actin levels are around 70. Compared to pre-stimulation, basal F-actin levels have increased and F-actin peaks in pseudopodia have decreased. The movement of the cell is very small, and nearly all nodes are stationary in Fig. 7B. The nearly uniform F-actin response at 8 s is transient; at 16 s the F-actin stain is uniformly low at about 40 arbitrary units (data not shown). The increase of myosin at the cortex that is observed at 20–30 s after cAMP stimulation is associated with enhanced retraction (data not shown). The perimeter of the cell has decreased slightly from 75 μm at −8 s to 71 μm at 8 s after stimulation. During the next 30 s the perimeter decreased steadily to 56 μm, due to the retraction of the pseudopodia while regions of extension remained absent.

The second F-actin response with maximum at 50–90 s after stimulation is associated with the extension of two new pseudopodia at 52 s. Interestingly, many changes in F-actin stain, myosin and movement of nodes are observed before the pseudopod is actually extended. Figure 7C demonstrates elevated F-actin levels at 44 s in three regions of the cell, which are the old (and future) uropod at perimeter 1, and two regions that will become pseudopodia at perimeter 0.3 and 0.6, respectively. Although these nodes exhibit elevated levels of F-actin, the nodes do not move yet. Four seconds later (48 s), the nodes associated with elevated F-actin and the future pseudopodia start to move, leading to a giant increase of the cell perimeter in the next frame (52 s, not shown) from 56 to 75 μm. Before movement starts (44 s), the levels of myosin II are relatively uniform and high around 60 arbitrary units. Interestingly, at 48 s, when

movement starts, myosin II levels in the region of movement have decrease considerably to around 30 (Fig. 7D). Figure 7E presents the area change, and levels of F-actin and myosin II in the two regions that form a pseudopod. Actin levels start to increase at 32 s after cAMP stimulation. Myosin II levels remain high, and movement of the nodes is essentially absent till 44 s. At 48 s myosin II levels decrease locally at the region of elevated F-actin stain, and at the same time the nodes are extended. We propose that the position of pseudopod extension at 52 s is determined much earlier, perhaps even before 30 s when F-actin starts to accumulate at those positions. We further propose that myosin filaments prevent extension of the F-actin rich regions, and that pseudopod extension is induced by local dissociation of myosin filaments at 48 s after cAMP stimulation. The present analysis was done in 2D on confocal sections, and does not take into account changes in the *Z*-direction. We expect that it will be difficult to implement 3D analysis, because the time required to obtain time series of images in the *Z*-direction induces phototoxicity. Probably 2D recording of cells with agar overlay is the best method to prevent major changes in the *Z*-direction.

The detailed analysis reveals that the first and second actin responses after uniform cAMP stimulation are very different. The first response is uniform, leading to retraction, possibly because the F-actin in the cortex is the matrix for acto-myosin mediated contraction. The second F-actin response is restricted to small areas of the cell, which, after disassembly of myosin filaments, leads to the extension of pseudopodia. The global correlation between extension/retraction with F-actin/myosin levels suggests that the observations made during the second actin response may represent the 'normal' mode of pseudopod extension.

CONCLUSIONS

Microscopy of cells expressing GFP-tagged proteins provides images with high spatial and temporal resolution. We developed improved Quimp2 software to simultaneously quantify local membrane movement and fluorescent intensities with similar high resolution. This will enable in depth analysis of the function of proteins in cell movement, and may help to answer important questions, such as which molecules determine the time and place of the initiation of a new pseudopod. Since cell movement is to a large extend stochastic, the identification of the underlying molecular mechanisms requires large data sets that can correlate local membrane movement with the intensities or activities of candidate proteins. Although written for the analysis of cell movement, the software is also applicable to other processes in cell biology, such as cell division [Müller-Taubenberger et al., 2002], organelle biogenesis or membrane fusion events.

REFERENCES

Berlot CH, Devreotes PN, Spudich JA. 1987. Chemoattractant elicited increases in Dictyostelium myosin phosphorylation are due to changes in myosin localization and increases in kinase activity. J Biol Chem 262:3918–3926.

Chen LF, Janetopoulos C, Huang YE, Iijima M, Borleis J, Devreotes PN. 2003. Two phases of actin polymerization display different dependencies on PI(3,4,5)P-3 accumulation and have unique roles during chemotaxis. Mol Biol Cell 14:5028–5037.

Dormann D, Libotte T, Weijer CJ, Bretschneider T. 2002. Simultaneous quantification of cell motility and protein-membrane-association using active contours. Cell Motil Cytoskeleton 52:221–230.

Etzrodt M, Ishikawa HC, Dalous J, Müller-Taubenberger A, Bretschneider T, Gerisch G. 2006. Time-resolved responses to chemoattractant, characteristic of the front and tail of Dictyostelium cells. FEBS Lett 580(28-29):6707–6713.

Fischer M, Haase I, Simmeth E, Gerisch G, Müller-Taubenberger A. 2004. A brilliant monomer red fluorescent protein to visualize cytoskeleton dynamics in Dictyostelium. FEBS Lett 577:227–232.

Hall AL, Schlein A, Condeelis J. 1988. Relationship of pseudopod extension to chemotactic hormone-induced actin polymerization in amoeboid cells. J Cell Biochem 37:285–299.

Kass M, Witkin A, Terzopoulos D. 1987. Snakes-active contour models. Int J Comput Vision 1:321–331.

Machacek M, Danuser G. 2006. Morphodynamic profiling of protrusion phenotypes. Biophys J 90(4):1439–1452.

McRobbie SJ, Newell PC. 1983. Changes in actin associated with the cytoskeleton following chemotactic stimulation of Dictyostelium discoideum. Biochem Biophys Res Commun 115:351–359.

McRobbie SJ, Newell PC. 1984. Chemoattractant-mediated changes in cytoskeletal actin of cellular slime moulds. J Cell Sci 68: 139–151.

Müller-Taubenberger A, Bretschneider T, Faix J, Konzok A, Simmeth E, Weber I. 2002. Differential localization of the Dictyostelium kinase DPAKa during cytokinesis and cell migration. J Muscle Res Cell Motil 23(7-8):751–763.

Prassler J, Murr A, Stocker S, Faix J, Murphy J, Marriott G. 1998. DdLIM is a cytoskeleton-associated protein involved in the protrusion of lamellipodia in Dictyostelium. Mol Biol Cell 9: 545–559.

Yumura S. 1994. Reorganization of actin and myosin II in Dictyostelium amoeba during stimulation by cAMP. Cell Struct Funct 18:379–388.

Yumura S, Mori H, Fukui Y. 1984. Localization of actin and myosin for the study of ameboid movement in Dictyostelium using improved immunofluorescence. J Cell Biol 99:894–899.